GREEN'S FUNCTIONS FOR POLYGONAL WAVEGUIDES BY THE RAY-OPTICAL TECHNIQUE

A Thesis

Presented To The

Faculty of Graduate Studies and Research

The University of Manitoba

In Partial Fulfillment

Of The Requirements For The Degree

Master of Science in Electrical Engineering

by

Wayne Arthur Johnson

July, 1967

ABSTRACT

The scalar and dyadic Green's functions for cavities and waveguides of various cross-sections are determined by the ray-optical technique. Simple ray tracing diagrams for parallel plate, rectangular and triangular waveguides and cavities are presented. The contributions due to all rays passing through an observation point are systematically summed and formally converted to a series of normal modes by the Poisson sum formula which is extended to two and three dimensions. The required Fourier transform of the ray field is evaluated by the stationary phase method of integration and the resulting Green's functions are shown to be in exact agreement with available results based on more complicated methods. This agreement is discussed with particular reference to the saddle point method of integration. It is also shown that the results for triangular waveguides, whose corner angles are integral submultiples of π , can be obtained by superposition of solutions for two rectangular waveguides. Finally, it is concluded that the ray-optical technique may lead to exact solutions for a more general class of waveguide structures and offers a physical insight into the mechanisms of wave propagation in waveguides of various cross-sections.

ACKNOWLEDGEMENTS

The author wishes to acknowledge the assistance given by Dr. M. A. K. Hamid who suggested the problem and supervised the work throughout.

Sincere thanks are also due to Dr. H. R. Coish of the Department of Physics and Dr. G. O. Martens of the Department of Electrical Engineering for their assistance. The author expresses his appreciation to Mrs. M. Cameron for the typing of the manuscript.

This research was supported by the Atomic Energy of Canada Ltd., Chemcell Ltd., and the National Research Council of Canada under grant A-3326.

TABLE OF CONTENTS

LIST OF FIGURES

CHAPTER I

INTRODUCTION

The Green's function is important in the study of boundary value problems in electromagnetics in the presence of an excitation system. Knowledge of this function leads easily to the solution for the electromagnetic field. This thesis is concerned with detailed applications of the ray and mode techniques for finding the Green's function in rectangular structures. The salient features of these methods are presented and their inter-relations discussed.

The investigation is restricted to cases in which the image method is applicable but the techniques used could easily be extended to include more complicated cases. Only rectangular coordinates are employed in the examples but the analysis applies to problems expressed in other coordinate systems.

The ray theory and mode theory solutions are related by the Poisson sum formula. This formula has been used by other authors[1, 2, 3] to convert from rays to modes and vice-versa. In this thesis, the Fourier transform involved in the Poisson formula is evaluated by asymptotic methods and agreement with mode theory solutions is obtained in all cases. This agreement is exact when dealing with the complex amplitudes of the transverse modes regardless of the asymptotic approximations involved.

CHAPTER II

DETERMINATION OF GREEN'S FUNCTIONS

One of the most powerful tools for solving boundary value problems involving excitation systems is the Green's function for the geometry of the problem. Two different methods for determining these functions are outlined and evaluated in this chapter.

2.1 Green's Functions

In this section, the Green's function due to a delta source, $\delta(\bar{r}-\bar{r}_o)$, where $\bar{r}$ and $\bar{r}_o$ correspond to the vector positions of the observation and source points respectively, is considered. For scalar problems the scalar Green's function, $G(\bar{r},\bar{r}_o)$, is used while for vector problems the dyadic Green's function, $\bar{\bar{G}}(\bar{r},\bar{r}_o)$, is used. These functions are obtained from the following forms of the Helmholtz equation:

$$(\nabla^2 + k^2)\, G(\bar{r},\bar{r}_o) = -4\pi\, \delta(\bar{r}-\bar{r}_o) \tag{2.1}$$

$$(\nabla^2 + k^2)\, \bar{\bar{G}}(\bar{r},\bar{r}_o) = -4\pi \bar{\bar{I}}\, \delta(\bar{r}-\bar{r}_o) \tag{2.2}$$

where $\bar{\bar{I}}$ is the unit idemfactor or dyadic analogue of unity (i.e. $\bar{\bar{I}} \cdot \bar{A} = \bar{A}$ where $\bar{A}$ is any vector), ∇^2 is the Laplacian operator, k is the wave number $(2\pi/\lambda)$, and λ is the wavelength in the medium concerned.

The above equations are used to solve for the Green's function subject to certain boundary conditions dictated by

the geometry of the problem. In order to simplify the solution for the fields, convenient boundary conditions on the Green's function are used, depending on the assumed boundary conditions for the field and the type of source.

A typical application of this function is the problem of determining the vector potential $\bar{A}(\bar{r})$ from an arbitrary current distribution $\bar{J}(\bar{r}_o)$ located in a volume V bounded by a surface S. $\bar{A}(\bar{r})$ is a solution of

$$\nabla^2 \bar{A} + k^2 \bar{A} = -\mu \bar{J}(\bar{r}_o). \tag{2.3}$$

Using the dyadic Green's function of equation (2.2) it is shown by Collin ,[4] and Morse and Feshbach[5] that the solution for $\bar{A}(\bar{r})$ is given by:

$$\bar{A}(\bar{r}) = \iiint_V \frac{\mu}{4\pi} \bar{J}(\bar{r}_o) \cdot \bar{\bar{\mathcal{G}}}(\bar{r},\bar{r}_o)\, dv_o$$

$$+ \frac{1}{4\pi} \oiint_S \left[(\hat{n} \times \bar{A}) \cdot (\nabla_o \times \bar{\bar{\mathcal{G}}}) + (\hat{n} \times \nabla_o \times \bar{A}) \cdot \bar{\bar{\mathcal{G}}} \right.$$

$$\left. + (\hat{n} \cdot \bar{A})(\nabla_o \cdot \bar{\bar{\mathcal{G}}}) - (\hat{n} \cdot \bar{\bar{\mathcal{G}}})(\nabla_o \cdot \bar{A}) \right] ds_o. \tag{2.4}$$

Here $\hat{n}$ is the inward normal to the volume and the integration is carried out over the source coordinates. Once the conditions on $\bar{A}$ over S are known, the surface integral can be eliminated by assuming convenient conditions on $\bar{\bar{\mathcal{G}}}$ over S. If the tangential electric field is zero over S it is easily shown that $\hat{n} \times \bar{A}$ and $\nabla_o \cdot \bar{A}$ are both zero there. When the conditions $\nabla_o \cdot \bar{\bar{\mathcal{G}}} = o$ and $\hat{n} \times \bar{\bar{\mathcal{G}}} = o$ over S are specified,

equation (2.4) simplifies to:

$$\bar{A}(\bar{r}) = \iiint_V \frac{\mu}{4\pi} \bar{J}(\bar{r}_o) \cdot \bar{\bar{\mathcal{G}}}(\bar{r},\bar{r}_o)\, dv_o. \qquad (2.5)$$

The electric and magnetic fields $(\bar{E},\bar{H})$ are easily derived from the vector potential through the relations:

$$\bar{E} = -j\omega\bar{A} + \frac{\nabla(\nabla \cdot \bar{A})}{j\omega\mu\epsilon} \qquad (2.6)$$

$$\bar{H} = \frac{1}{\mu} \nabla \times \bar{A}. \qquad (2.7)$$

Here μ and ϵ are the permeability and permittivity of the medium involved and ω is the radian frequency.

The free space Green's function may be applied to solve for the field in regions with complicated boundaries. When the boundaries are at infinity and a time dependence of $\exp(j\omega t)$ is assumed, the free space scalar Green's function, $G_k(\bar{r},\bar{r}_o)$, is easily determined as shown by Morse and Feshbach.[6] For waves extending outward from the source these functions are:

$$G_k(\bar{r},\bar{r}_o) = \frac{e^{-jk|\bar{r}-\bar{r}_o|}}{|\bar{r}-\bar{r}_o|} \text{ in three dimensions,} \qquad (2.8)$$

$$G_k(\bar{r},\bar{r}_o) = j\pi H_o^{(2)}(k|\bar{r}-\bar{r}_o|) \text{ in two dimensions,} \qquad (2.9)$$

$$G_k(\bar{r},\bar{r}_o) = \frac{2\pi j}{k} e^{-jk|x-x_o|} \text{ in one dimension.} \qquad (2.10)$$

The free space solution of equation (2.2) is

determined from the scalar solution by using the relationship:

$$\bar{\mathcal{G}}_k(\bar{r},\bar{r}_o) = G_k(\bar{r},\bar{r}_o)\bar{\mathcal{J}}. \tag{2.11}$$

2.2 Image Method

"The image method is a method for constructing a Green's function for a part of space bounded by planes in terms of the corresponding Green's function for the full space." This is shown in an article[7] by J. B. Keller who has determined all the regions, equations, and boundary conditions to which the image method may be applied.

For a region D bounded by planes on which homogeneous boundary conditions are specified, $G(\bar{r},\bar{r}_o)$ is given in terms of $G_k(\bar{r},\bar{r}_o)$ by forming the sum:

$$G(\bar{r},\bar{r}_o) = \sum_{\bar{r}_o' \in S(\bar{r}_o)} (\pm)\, G_k(\bar{r},\bar{r}_o'). \tag{2.12}$$

Here $S(r_o)$ is a set made up of the source, its images, and the multiple images in the bounding planes of D. The positive and negative signs in equation (2.12) correspond to the Neumann ($\partial G/\partial n = o$) and Dirichlet ($G = o$) boundary conditions, respectively.

The conditions and regions to which the image method may be applied are as follows:

(1) $S(\bar{r}_o)$ has only one point, $\bar{r}_o$ itself, in D.

(2) Only those fundamental domains of discrete groups of reflections for which the angle between any two bounding planes is of the form π/m, with m integral, can be admissible regions.

(3) The angles between planes on which the Dirichlet condition is imposed and those on which the Neumann condition is imposed must be even submultiples of π.

(4) $\nabla^2 + k^2$ is a valid operator for the image method.

The preceeding method can be extended to determine the dyadic Green's function for a vector current source in an arbitrarily bounded region. It can easily be shown that the conditions on $\bar{\bar{\mathcal{G}}}(\bar{r},\bar{r}_o)$ preceeding equation (2.5) imply an image diagram as shown in Figure 2.1 for the specific case of a vector current source $\bar{J}(\bar{r}_o)$ located in the presence of a perfectly conducting plane.[4] Here it is noted that the component of $\bar{J}(\bar{r}_o)$ parallel to the plane has a negative image and the perpendicular component has a positive image. In general, to find the field due to an arbitrarily oriented source, $\bar{J}(\bar{r}_o)$, is decomposed into its components parallel and perpendicular to the boundary and scalar theory is used for each component and its images. The principle of superpositionis invoked to determine the dyadic Green's function. Once $\bar{\bar{\mathcal{G}}}(\bar{r},\bar{r}_o)$ has been found, the fields are given by equations (2.5), (2.6), and (2.7) for an arbitrary current source.

The image method may be used to construct ray

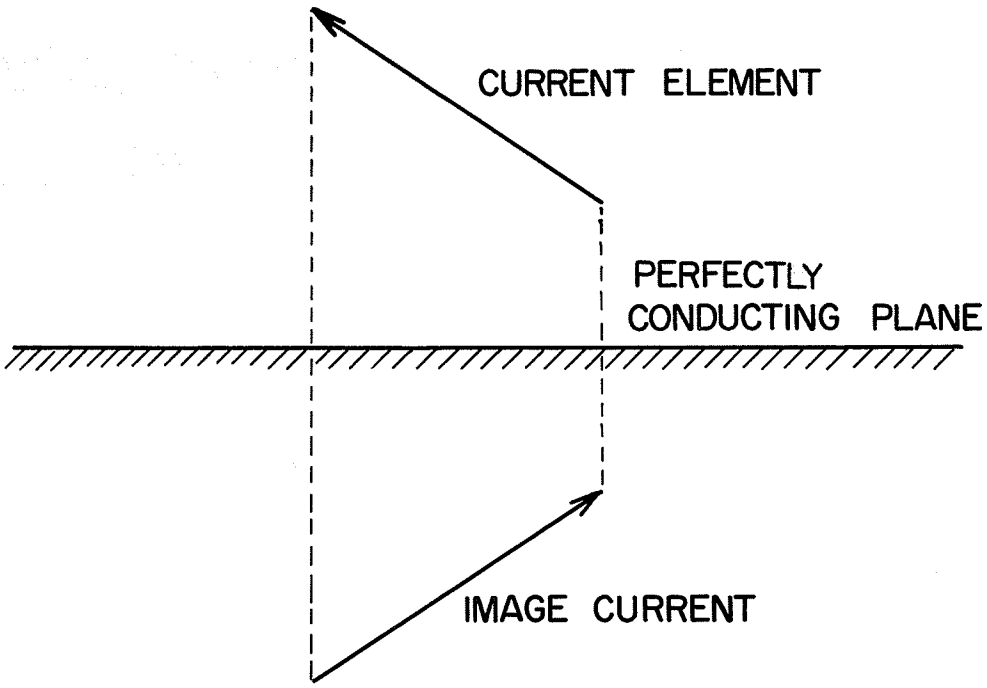

FIGURE 2-1

CURRENT SOURCE IMAGE DIAGRAM

diagrams in geometrical configurations where the location of the source and nature of the scattering boundaries are given. Viewed in this way, the method of successive images can complement the ray technique by Keller[8] and provide a solution to fields within such boundaries as specified by the scope of the image method. Since it may be shown that diffraction losses are not present in the particular configurations under consideration, Keller's technique reduces in such cases to the classical geometrical optics method.

2.3 The Eigenfunction Method

It is well known that a series of eigenfunctions can be used to represent the solution of boundary value problems. In general, eigenfunctions are solutions of differential equations containing a separation constant and satisfying simple boundary conditions related to the independent variable. The values of the separation constant for which the boundary conditions hold are called eigenvalues. While the solution of boundary value problems can be written as a series of such functions, the difficulty still lies in finding the coefficients of the series. The constants in the series are usually determined using the orthogonality property of the eigenfunctions. This leads to integrals which may be evaluated exactly only for specific problems with simple geometries.

The application of vector eigenfunctions to the determination of dyadic Green's functions has been considered extensively by Morse and Feshbach.[5] Briefly the technique consists of expanding $\bar{\bar{\mathcal{G}}}(\bar{r},\bar{r}_o)$ for the interior of a closed boundary in terms of eigenvectors. It can be shown that the following relationship holds:

$$\bar{\bar{\mathcal{G}}}(r,r_o) = 4\pi \sum_n \frac{\bar{F}_n^*(\bar{r})\, \bar{F}_n(\bar{r}_o)}{\Lambda_n (k_n^2 - k^2)} . \tag{2.13}$$

Here $\bar{F}_n$ is an eigenfunction solution of the homogeneous vector Helmholtz equation satisfying the same homogeneous conditions as $\bar{\bar{\mathcal{G}}}(\bar{r},\bar{r}_o)$, k_n is its eigenvalue, Λ_n is a normalizing constant, and $\bar{F}_n^*$ is the complex conjugate of $\bar{F}_n$. The product $\bar{F}_n^*(\bar{r})\, \bar{F}_n(\bar{r}_o)$ results in a dyadic.[9]

The eigenfunction $\bar{F}_n$ can be expanded as a sum of longitudinal and transverse modes in the form:

$$\bar{F}_n = \bar{L}_n + \bar{M}_n + \bar{N}_n . \tag{2.14}$$

The functions $\bar{L}_n$, $\bar{M}_n$, and $\bar{N}_n$ are determined from eigenfunction solutions of the corresponding scalar equation. These functions have been derived for various sets of boundary conditions by Morse and Feshbach and are used to find the Green's function for a rectangular cavity in Chapter IV.

CHAPTER III

RAY THEORY VS. MODE THEORY

It has been shown that the ray and eigenfunction methods can be used to solve boundary value problems. The methods differ greatly in their application and the form in which the final solution appears. The relative merits of the two techniques and the conversion from one form of solution to the other are discussed in this chapter.

3.1 Rays and Modes

The Green's function defined in Chapter II can be expressed in two distinct ways, either as a sum of normal modes or as a sum of rays. In general, the normal modes are determined by solving the appropriate partial differential equation while the ray solution is formed using Keller's geometrical theory of diffraction. The eigenfunction method is applied easily only to those coordinate systems in which the differential equation is separable and the boundaries coincide with coordinate surfaces. The ray method does not have this restriction but it yields only the first term in the asymptotic expansion of the mode solution. The accuracy of this approach improves as the wave number k and the distance of the observation point from the source increase.

The total field due to all the modes present in a system is asymptotically equal to the total field on all

the rays provided that the field is time harmonic. The exception to this, as will be shown later, is the case where the image method applies and the ray solution for a point source bounded by perfect conductors is exact. Here the ray and mode representations are equivalent and one form can be converted to the other by various mathematical techniques. The transformation of modes to rays and vice-versa can be done for the general case as well, but the agreement is only an asymptotic one.

Hamid[1] has used both the Poisson sum formula and the Fourier-Bessel series to express asymptotic ray fields as a series of wave functions in the solution of near field transmission problems. Brekhovskikh[10] and Pekeris[2] have used the Poisson sum formula in the form derived by Titchmarsh[11] to change the normal mode solution into the ray solution. Their work has been confined to media with infinite parallel boundaries. Brekhovskikh was able to transform from rays to modes by expanding the term $\exp(jkR)/R$ in a contour integral form and then using the residue theorem. The procedure is quite complicated and so far has only been applied to the parallel plate case. Morse and Feshbach[12] used a slightly different form of the Poisson sum formula to convert from an image formulation for a line source between parallel plates to the mode form. The form of the Poisson sum formula used by Morse and Feshbach is used in this thesis to determine the mode

solution from the ray formulation for sources located inside rectangular waveguides and cavities.

3.2 Poisson Sum Formula

The Poisson sum formula has been widely applied to convert one infinite series into another. It is most useful when one transforms a slowly converging series to a more rapidly converging one. It was derived for a single infinite series but it can be extended to deal with double and triple summations as is shown in Appendix A.

The Poisson sum formula applied to a single infinite series is given by:

$$\sum_{n=-\infty}^{\infty} f(2\pi n) = \frac{1}{\sqrt{2\pi}} \sum_{m=-\infty}^{\infty} F(m) \tag{3.1}$$

where

$$F(m) = \frac{1}{\sqrt{2\pi}} \int_{-\infty}^{\infty} f(t)\, e^{-jmt}\, dt. \tag{3.2}$$

An extension to three dimensions as in Appendix A results in:

$$\sum_{n} \sum_{p} \sum_{q} f(2\pi n, 2\pi p, 2\pi q)$$

$$= \sum_{m} \sum_{s} \sum_{u} \frac{1}{(2\pi)^3} \int_{-\infty}^{\infty}\int_{-\infty}^{\infty}\int_{-\infty}^{\infty} f(t_1,t_2,t_3) \cdot$$

$$e^{-j(mt_1 + st_2 + ut_3)}\, dt_1 dt_2 dt_3 \tag{3.3}$$

where the summation signs extend over the infinite ranges of n, p, q, m, s, and u.

When equation (3.3) is applied to ray and mode representations of fields, the left hand side is the sum of the ray fields due to a triply infinite number of images and the right hand side represents the sum of all the possible modes which can exist to make up the total field. Each mode has associated with it one value of each of m, s, and u while the values of n, p, and q are identified with the source and all of its images.

The main difficulty in applying this method is the evaluation of the Fourier transform of the ray fields. The single integral transform has been done exactly by Morse and Feshbach[3] for the case of a line source exciting a parallel plate system by expressing the integrand in an integral form and then using the residue theorem. The case of a point source between parallel plates was done in a similar manner by Brekhovskikh.[10] The application of the Poisson formula to more complicated problems is possible since the Fourier transform can be evaluated using the principle of stationary phase method of integration. The result obtained by this technique is normally the first term of the asymptotic expansion of the exact solution. Under certain conditions the method does result in exact solutions and these cases are the subject of later chapters.

3.3 Principle of Stationary Phase

The principle of stationary phase asserts that as k goes to infinity, the dominant terms in the asymptotic expansion of the integral

$$\int_{-\infty}^{\infty} e^{jkg(t)} f(t)\, dt$$

where g(t) is real, arise from the immediate neighborhoods of the points at which the phase kg(t) is stationary. The method was first used by Lord Kelvin and later by numerous authors such as Copson,[13] Erdelyi,[14] and Felsen and Marcuvitz[15]. The method is developed in great detail by these authors and hence only the results are presented here.

The formula which applies to the cases dealt with in this thesis is:

$$\int_{-\infty}^{\infty} f(t)\, e^{jkg(t)}\, dt \simeq \left[\frac{2}{k|g''(t_o)|}\right]^{1/2} f(t_o)\, e^{jkg(t_o) \pm j\frac{\pi}{4}} + O\left(\frac{1}{k}\right). \qquad (3.4)$$

The stationary phase point, t_o is found by setting $g'(t_o) = o$ where the prime denotes differentiation with respect to t. The plus and minus signs in the exponent hold for $g''(t_o) > o$ and $g''(t_o) < o$, respectively. If $g''(t_o) = o$ the form of the approximation is changed and equation (3.4) is invalid. The product of k times the remainder in the expansion is bounded by a constant.

For multiple integrals equation (3.4) can be applied successively. In general, for a double integral the following formula has been derived as shown by Born and Wolf[16] and can thus be applied directly to the problem as shown in Chapter IV:

$$\int_{-\infty}^{\infty}\int_{-\infty}^{\infty} f(x,y)\, e^{jkg(x,y)}\, dxdy \sim \frac{2\pi j\,\sigma}{[|\alpha\beta-\gamma^2|]^{1/2}} \cdot f(x_o,y_o)\, \frac{e^{jkg(x_o,y_o)}}{k} \qquad (3.5)$$

where

$$\sigma = \begin{cases} +1 & \alpha\beta > \gamma^2, \quad \alpha > 0 \\ -1 & \alpha\beta > \gamma^2, \quad \alpha < 0 \\ -j & \alpha\beta < \gamma^2 \end{cases}$$

$$\alpha = \frac{\partial^2 g}{\partial x^2}\bigg|_{(x_o,y_o)} \qquad \beta = \frac{\partial^2 g}{\partial y^2}\bigg|_{(x_o,y_o)} \qquad \gamma = \frac{\partial^2 g}{\partial x \partial y}\bigg|_{(x_o,y_o)}$$

$\frac{\partial g}{\partial x} = \frac{\partial g}{\partial y} = 0$ at the point (x_o,y_o).

CHAPTER IV

SOLUTION FOR GREEN'S FUNCTION IN RECTANGULAR STRUCTURES

The techniques described in Chapters II and III are easily applied to wave propagation in rectangular structures. We assume that all bounding planes are perfectly conducting so that simple image diagrams result. The image method is used to find the ray fields from a point source in a parallel plate waveguide, a rectangular waveguide, a shorted waveguide, and a rectangular cavity. In this order, the formulation varies from the simple case of a single infinite sum to the rather more lengthy triple summation. The ray fields are expressed in terms of mode fields by using the Poisson sum formula discussed previously. These examples require the use of the one, two, and three dimensional Fourier transform of the ray fields. The evaluation of these integrals is done in all cases by the principle of stationary phase. The results are found to be in exact agreement with available solutions for most cases considered.

4.1 Ray Solution for a Parallel Plate Waveguide

The simplest case to discuss first is that of a point source between parallel plates located at $x = o$ and $x = a$ in the $y - z$ plane of a rectangular coordinate system as shown in Figure 4.1. The source and observation points are

located at (x_o, y_o, z_o) and (x, y, z), respectively. Application of the image method to the determination of the scalar Green's function, $G(\bar{r},\bar{r}_o)$ for the boundary condition $G = o$ at $x = o, a$ results in the image diagram also shown in Figure 4.1. There are positive images at $Rn^+ = \{[x - (2na + x_o)]^2 + r^2\}^{1/2}$ and negative images at $Rn^- = \{[x - (2na - x_o)]^2 + r^2\}^{1/2}$, where n varies from minus infinity to plus infinity through integer values and where $r^2 = (y - y_o)^2 + (z - z_o)^2$. Adding the contributions from all the images yields:

$$G(\bar{r},\bar{r}_o) = \sum_{n=-\infty}^{\infty} \left\{ \frac{e^{-jkRn^+}}{Rn^+} - \frac{e^{-jkRn^-}}{Rn^-} \right\}. \qquad (4.1)$$

Equation (4.1) is the basic solution for the problem by the ray method. In order to convert the sum of rays into a series of normal modes the Poisson sum formula is used in the following manner. $Rn^{\pm}$ is first written as a function $2\pi n$ or t and equations (3.1) and (3.2) are applied to equation (4.1). The Fourier integral to be evaluated is given by:

$$F^{\pm}(m) = \frac{1}{\sqrt{2\pi}} \int_{-\infty}^{\infty} \frac{e^{-jk\left[r^2 + (x \mp x_o - \frac{ta}{\pi})^2\right]^{1/2} - jmt}}{\left[r^2 + (x \mp x_o - \frac{ta}{\pi})^2\right]^{1/2}} dt. \qquad (4.2)$$

The expression for the Green's function is thus given by:

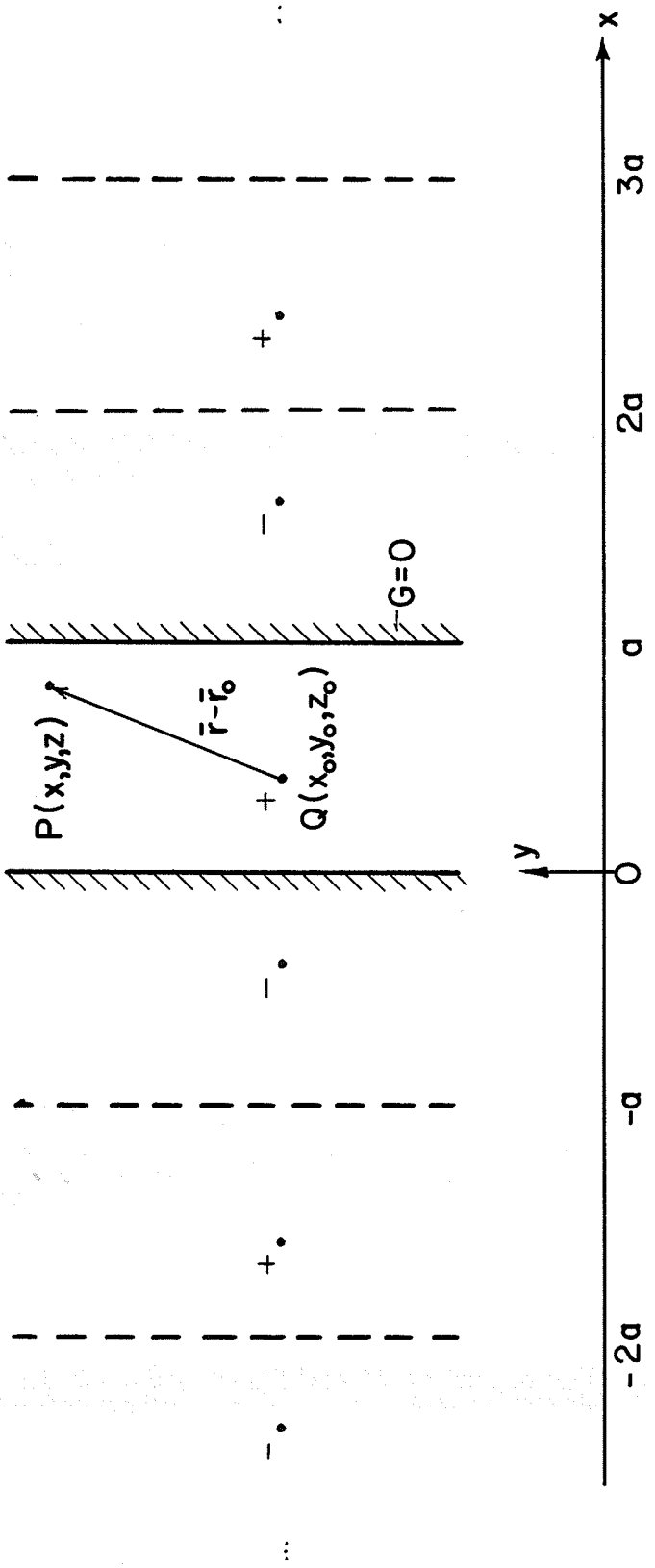

FIGURE 4.1

IMAGE DIAGRAM FOR A PARALLEL PLATE WAVEGUIDE

$$G(\bar{r},\bar{r}_o) = \sum_{m=-\infty}^{\infty} \frac{1}{\sqrt{2\pi}} \left\{ F^{+}(m) - F^{-}(m) \right\}. \qquad (4.3)$$

Since the integral in equation (4.2) is rather difficult to evaluate exactly, an asymptotic approach is used. The application of the principle of stationary phase to the integral results in a stationary phase point at

$$t_o = \frac{\pi}{a} \left\{ x \mp x_o - \frac{r}{\left[\left(\frac{ka}{m\pi} \right)^2 - 1 \right]^{1/2}} \right\}. \qquad (4.4)$$

Using the formulation given in Chapter III the expression for $F^{\pm}(m)$ is thus:

$$F^{\pm}(m) = \frac{\pi}{a\,(\beta r)^{1/2}}\, e^{-j\frac{m\pi}{a}(x \mp x_o) - j\beta r - j\frac{\pi}{4}} \qquad (4.5)$$

where $$\beta^2 = k^2 - \left(\frac{m\pi}{a} \right)^2 . \qquad (4.6)$$

After some simplification, the Green's function is found to be:

$$G(\bar{r},\bar{r}_o) \sim -2j\frac{\pi}{a} \sum_{m=1}^{\infty} \left[\frac{2}{\pi\beta r} \right]^{1/2} e^{-j\beta r + j\frac{\pi}{4}} \sin \frac{m\pi x}{a} \cdot \sin \frac{m\pi x_o}{a} . \qquad (4.7)$$

A similar formulation of this problem was done by Pekeris.[2] He was able to evaluate both the ray and mode solutions exactly and convert one to the other using

integral forms of the functions involved and the techniques of contour integration. His mode solution is given by:

$$G(\bar{r},\bar{r}_o) = -2j \frac{\pi}{a} \sum_{m=1}^{\infty} H_o^{(2)} (\beta r) \sin \frac{m\pi x}{a} \sin \frac{m\pi x_o}{a} . \quad (4.8)$$

The right hand side of equation (4.7) is the first term in the asymptotic expansion of the exact solution given by equation (4.8). This result is expected since the principle of stationary phase yields the first term in the asymptotic expansion of the integral to which it is applied.

4.2 Ray Solution for a Rectangular Waveguide

The response of a waveguide to a current source can be easily determined by the method outlined previously. For a current source the Green's function corresponding to the vector potential $\bar{A}$ must be found. From this the electric and magnetic fields are easily derived. The image method is used here to find the ray solution in the same manner as in the parallel plate case.

For the sake of simplicity we assume a y - directed infinitesimal current element located at the point (x_o, y_o, z_o) in a rectangular waveguide of dimensions a and b as shown in Figure 4.2. There is no loss of generality in this assumption since any arbitrary orientation of a current source can be handled by superimposing the effects of three component sources along mutually perpendicular axes. For

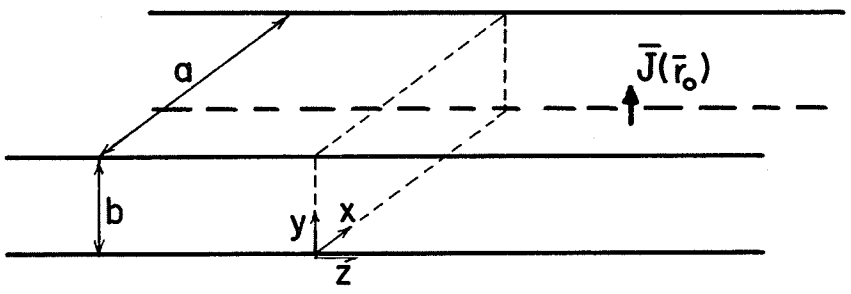

FIGURE 4.2

CURRENT ELEMENT IN A RECTANGULAR WAVEGUIDE

the condition of zero tangential electric field at the guide walls, the Green's function for the y - directed current element must satisfy the Dirichlet boundary condition ($G = o$) in the y - z plane and the Neumann condition ($\partial G/\partial n = o$) in the x - z plane. Using the image diagram shown in Figure 4.3, the solution for $G(\bar{r},\bar{r}_o)$ is easily written as:

$$G(\bar{r},\bar{r}_o) = \sum_{n=-\infty}^{\infty} \sum_{p=-\infty}^{\infty} \left[\frac{e^{-jkR_1}}{R_1} - \frac{e^{-jkR_2}}{R_2} + \frac{e^{-jkR_3}}{R_3} - \frac{e^{-jkR_4}}{R_4} \right] \quad (4.9)$$

where

$$R_1^2 = (x - x_o - 2na)^2 + (y - y_o - 2pb)^2 + (z - z_o)^2$$

$$R_2^2 = (x + x_o - 2na)^2 + (y - y_o - 2pb)^2 + (z - z_o)^2$$

$$R_3^2 = (x - x_o - 2na)^2 + (y + y_o - 2pb)^2 + (z - z_o)^2$$

$$R_4^2 = (x + x_o - 2na)^2 + (y + y_o - 2pb)^2 + (z - z_o)^2.$$

When the Poisson sum formula is applied to convert this to a mode solutinn a double integral of the following form results:

$$\int_{-\infty}^{\infty} \int_{-\infty}^{\infty} \frac{e^{-jk\left[(x\mp x_o-2na)^2 + (y\mp y_o-2pb)^2 + (z-z_o)^2\right]^{1/2}}}{\left[(x\mp x_o-2na)^2 + (y\mp y_o-2pb)^2 + (z-z_o)^2\right]^{1/2}} \cdot$$

$$e^{-j(mt_1+st_2)}\, dt_1 dt_2. \quad (4.10)$$

Application of the stationary phase formula given in

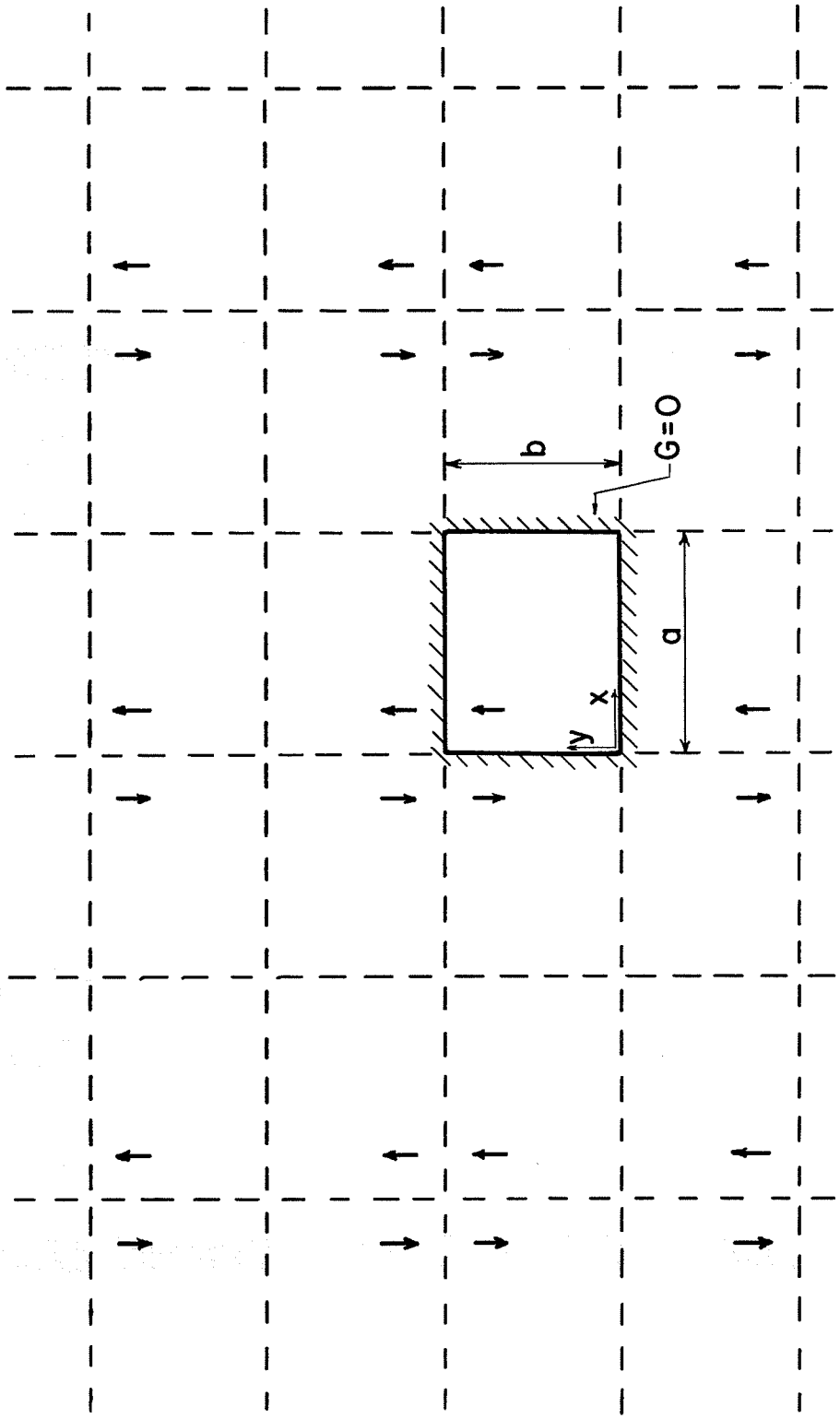

FIGURE 4.3

IMAGE DIAGRAM FOR A RECTANGULAR WAVEGUIDE

equation (3.5) results in the following expression as shown in Appendix B:

$$G(\bar{r},\bar{r}_o) = \frac{-4\pi j}{ab} \sum_{s=o}^{\infty} \sum_{m=1}^{\infty} \frac{\epsilon_s}{\beta_2} e^{-j\beta_2|z-z_o|} \cdot$$

$$\sin \frac{m\pi x_o}{a} \cos \frac{s\pi y_o}{b} \sin \frac{m\pi x}{a} \cos \frac{s\pi y}{b} \qquad (4.11)$$

where

$$\epsilon_s = \begin{cases} 1 & s = o \\ 2 & s \neq o \end{cases}$$

$$\beta_2^2 = k^2 - \left(\frac{m\pi}{a}\right)^2 - \left(\frac{s\pi}{b}\right)^2 .$$

In order to compare with available results, the electric field is calculated using equations (2.5) and (2.6) for a current element of length b exciting the TE_{mo} modes. The electric field determined in this manner is:

$$Ey = - \frac{\omega\mu}{a} \sum_{m=1}^{\infty} \frac{1}{\beta_2} \sin \frac{m\pi x}{a} \sin \frac{m\pi x_o}{a} e^{-j\beta_2|z-z_o|} \qquad (4.12)$$

Since the only possible solution for such a current element corresponds to s = o, the expression for β_2 is then given by:

$$\beta_2^2 = k^2 - \left(\frac{m\pi}{a}\right)^2 \qquad (4.13)$$

Equation (4.12) agrees then exactly with Collin's[17] result

for the same problem.

4.3 Ray Solution for a Shorted Waveguide

As another test case, we apply the ray method to a waveguide with a shorting plate placed at the cross section $z = o$ in order to determine the Green's function in the guide for $z > o$. The source is again located at (x_o, y_o, z_o). The resulting image diagram is identical to the previous case except for the additional images in the $x - y$ plane at $z = -z_o$ due to the shorting plate. The new images are of opposite polarity due to the boundary condition at the plane $z = o$. The required solution is given by the difference of two terms, each identical to the right hand side of equation (4.11) except that the sign of z_o is reversedin the second term. The Green's function for this problem is then:

$$G(\bar{r},\bar{r}_o) = -\frac{4\pi j}{ab} \sum_{m=1}^{\infty} \sum_{s=o}^{\infty} \frac{\epsilon_s}{2} \sin \frac{m\pi x_o}{a} \cos \frac{s\pi y_o}{b} \cdot$$

$$\sin \frac{m\pi x}{a} \cos \frac{s\pi y}{b} \left\{ e^{-j\beta_2 |z-z_o|} - e^{-j\beta_2 |z+z_o|} \right\}. \qquad (4.14)$$

After some simplification, the final solution is given by:

$$G(\bar{r},\bar{r}_o) = \frac{8\pi}{ab} \sum_{m=1}^{\infty} \sum_{s=o}^{\infty} \epsilon_s \sin \frac{m\pi x_o}{a} \cos \frac{s\pi y_o}{b} \cdot$$

$$\sin \frac{m\pi x}{a} \quad \cos \frac{s\pi y}{b} \begin{cases} e^{-j\beta_2 z} \sin \beta_2 z & z \geq z_o \\ e^{-j\beta_2 z_o} \sin \beta_2 z & z \leq z_o \end{cases} \quad (4.15)$$

This is exactly the Green's function derived directly from mode theory as shown by Collin.[18]

4.4 Ray Solution for a Rectangular Cavity

The previous solutions can be easily extended to consider the dyadic Green's function for an arbitrary current source in a rectangular cavity. For this we obtain a general solution of equation (2.2) with the particular condition of zero tangential electric field on the bounding planes.

The excitation of a cavity by an arbitrary current element, $\bar{J}(\bar{r}_o)$ can be split up into the responses due to each of the components of $\bar{J}(\bar{r}_o)$ along the three coordinate axes. Since the final solution is obtained by superposition, we need to consider only the response to a y - directed current element. The image diagram is then the same as that shown in Figure 4.3. There are similar diagrams for all the x - y planes at which $z = 2qd \pm z_o$, where d is the z - dimension of the cavity and q is any integer. By summing the contributions from all the images the following expression results for the $\hat{j}\hat{j}$ component of $\bar{\bar{G}}_e(\bar{r},\bar{r}_o)$:

$$G_y = \sum_{n=-\infty}^{\infty} \sum_{p=-\infty}^{\infty} \sum_{q=-\infty}^{\infty} \left\{ \sum_{\ell=1}^{8} (-1)^{\ell+1} \frac{e^{-jkR_\ell}}{R_\ell} \right\} \qquad (4.16)$$

where

$$R_\ell^2 = (x_\ell - 2na)^2 + (y_\ell - 2pb)^2 + (z_\ell - 2qd)^2$$

$$x_\ell = \begin{cases} x - x_o & \ell = 1, 3, 6, 8 \\ x + x_o & \ell = 2, 4, 5, 7 \end{cases}$$

$$y_\ell = \begin{cases} y - y_o & \ell = 1, 2, 5, 6 \\ y + y_o & \ell = 3, 4, 7, 8 \end{cases}$$

$$z_\ell = \begin{cases} z - z_o & \ell = 1, 2, 3, 4 \\ z + z_o & \ell = 5, 6, 7, 8 \end{cases}$$

A typical term in the above summation has the form:

$$\sum_n \sum_p \sum_q \frac{e^{-jk\left[(x_\ell - 2na)^2 + (y_\ell - 2pb)^2 + (z_\ell - 2qd)^2\right]^{1/2}}}{\left[(x_\ell - 2na)^2 + (y_\ell - 2pb)^2 + (z_\ell - 2qd)^2\right]^{1/2}} . \qquad (4.17)$$

Application of the Poisson sum formula of equation (3.3) leads to the following three dimensional Fourier integral:

$$\frac{1}{(2\pi)^3} \int_{-\infty}^{\infty} \int_{-\infty}^{\infty} \int_{-\infty}^{\infty} \frac{e^{-jk\left[(x_\ell - t_1 \frac{a}{\pi})^2 + (y_\ell - t_2 \frac{b}{\pi})^2 + (z_\ell - t_3 \frac{d}{\pi})^2\right]^{1/2}}}{\left[(x_\ell - t_1 \frac{a}{\pi})^2 + (y_\ell - t_2 \frac{b}{\pi})^2 + (z_\ell - t_3 \frac{d}{\pi})^2\right]^{1/2}} \cdot$$

$$e^{-j(mt_1 + st_2 + ut_3)} \, dt_1 dt_2 dt_3 . \qquad (4.18)$$

Integrals of this type may be evaluated by application of the principle of stationary phase with respect to t_1 and t_2 as shown in Appendix B. This reduces the integral of (4.18) to the following form:

$$\frac{-j}{4ab\beta_2} e^{-j\left(\frac{m\pi x_\ell}{a}+\frac{s\pi y_\ell}{b}\right)} \int_{-\infty}^{\infty} e^{-j\beta_2\left|z_\ell-t_3\frac{d}{\pi}\right|-jut_3}\, dt_3 \qquad (4.19)$$

where $$\beta_2^2 = k^2 - \left(\frac{m\pi}{a}\right)^2 - \left(\frac{s\pi}{b}\right)^2.$$

The integration over t_3 can be achieved by splitting the range of integration as shown in Appendix C. The typical term given by (4.17) is then written as:

$$\frac{\pi}{2abd} \sum_{m=-\infty}^{\infty} \sum_{s=-\infty}^{\infty} \sum_{u=-\infty}^{\infty} \frac{e^{-j\left(\frac{m\pi x_\ell}{a}+\frac{s\pi y_\ell}{b}+\frac{u\pi z_\ell}{d}\right)}}{\left(\frac{u\pi}{d}\right)^2-\beta_2^2}. \qquad (4.20)$$

The triple sum of (4.20) may be interpreted as the sum of plane waves which, when combined according to equation (4.16), results in the Green's function for the cavity. By proper substitution of the variables x_ℓ, y_ℓ, and z_ℓ and by changing the limits of summation, the Green's function is found to be:

$$G_y(\bar{r},\bar{r}_o) = \frac{16\pi}{abd} \sum_{m=1}^{\infty} \sum_{s=o}^{\infty} \sum_{u=1}^{\infty} \frac{\epsilon_s}{\left(\frac{u\pi}{d}\right)^2-\beta_2^2}.$$

$$\sin \frac{m\pi x_o}{a} \quad \sin \frac{m\pi x}{a} \quad \cos \frac{s\pi y_o}{b} \cos \frac{s\pi y}{b} \sin \frac{u\pi z_o}{d} \cdot$$

$$\sin \frac{u\pi z}{d} \cdot \qquad (4.21)$$

The complete dyadic Green's function is determined by repeating the above procedure for the cases of an x - directed and a z - directed current element and then applying superposition. By symmetry it is easily seen that the final expression is:

$$\bar{\mathcal{G}}(\bar{r},\bar{r}_o) = \frac{4\pi}{abd} \sum_{m=o}^{\infty} \sum_{s=o}^{\infty} \sum_{u=o}^{\infty} \frac{\epsilon_s \epsilon_m \epsilon_u}{(\frac{u\pi}{d})^2 - \beta_2^2} \cdot$$

$$\left[\cos \frac{m\pi x_o}{a} \cos \frac{m\pi x}{a} \sin \frac{s\pi y_o}{b} \sin \frac{s\pi y}{b} \sin \frac{u\pi z}{d} \sin \frac{u\pi z_o}{d} \hat{i}\hat{i} \right.$$

$$+ \sin \frac{m\pi x_o}{a} \sin \frac{m\pi x}{a} \cos \frac{s\pi y_o}{b} \cos \frac{s\pi y}{b} \sin \frac{u\pi z}{d} \sin \frac{u\pi z_o}{d} \hat{j}\hat{j}$$

$$\left. + \sin \frac{m\pi x_o}{a} \sin \frac{m\pi x}{a} \sin \frac{s\pi y_o}{b} \sin \frac{s\pi y}{b} \cos \frac{u\pi z_o}{d} \cos \frac{u\pi z}{d} \hat{k}\hat{k} \right] \qquad (4.22)$$

where

$$\epsilon_{m,s,u} = \begin{cases} 1 & u,\ s,\ m = o \\ 2 & u,\ s,\ m \neq 0 \end{cases}$$

Equation (4.22) is in exact agreement with the solution based on the eigenfunction method as shown in the next section.

4.5 Eigenfunction Solution for a Rectangular Cavity

The dyadic Green's function is a solution of equation (2.2) and it has been shown[5] that if $\bar{F}_n$ is an eigenfunction solution of

$$\nabla^2\bar{F}_n + k^2\bar{F}_n = o \tag{4.23}$$

and satisfies the same homogeneous conditions as $\bar{\bar{\mathcal{G}}}(\bar{r},\bar{r}_o)$, then $\bar{\bar{\mathcal{G}}}(\bar{r},\bar{r}_o)$ can be written as:

$$\bar{\bar{\mathcal{G}}}(\bar{r},\bar{r}_o) = 4\pi \sum_n \frac{\bar{F}_n^*(\bar{r})\,\bar{F}_n(\bar{r}_o)}{\Lambda_n (k_n^2-k^2)} \tag{4.24}$$

where the normalizing constant Λ_n is given by:

$$\iiint_V \bar{F}_n^* \cdot \bar{F}_m \, dv = \begin{cases} \Lambda_n & m = n \\ o & m \neq n \ . \end{cases} \tag{4.25}$$

The total Green's function for the rectangular cavity can be expressed as the sum of longitudinal and transverse parts, i.e.:

$$\bar{\bar{\mathcal{G}}}(\bar{r},\bar{r}_o) = 4\pi \sum_n \left\{ \frac{\bar{L}_n^*(\bar{r})\,\bar{L}_n(\bar{r}_o)}{\Lambda_n(k_n^2-k^2)} + \frac{\bar{M}_n^*(\bar{r})\,\bar{M}_n(\bar{r}_o)}{\Lambda_n'(k_n^2-k^2)} + \frac{\bar{N}_n^*(\bar{r})\,\bar{N}_n(\bar{r}_o)}{\Lambda_n''(k_n^2-k^2)} \right\} \tag{4.26}$$

where

$$\bar{F} = \bar{L} + \bar{M} + \bar{N} \tag{4.27}$$

The functions $\bar{L}$, $\bar{M}$, and $\bar{N}$ are given by Morse and Feshbach[5] for various sets of boundary conditions. The set of eigenfunctions satisfying the boundary conditions

$$\nabla \cdot \bar{F} = \hat{n} \times \bar{F} = o \tag{4.28}$$

is given by the following equations:

$$\bar{L}_n = \frac{m\pi}{a} \bar{U} + \frac{s\pi}{b} \bar{V} + \frac{u\pi}{d} \bar{W} \tag{4.29}$$

$$\bar{M}_n = \frac{-u\pi}{d} \bar{V} + \frac{s\pi}{b} \bar{W} \tag{4.30}$$

$$\bar{N}_n = \frac{\pi^2}{k_n}\left[\left(\frac{s}{b}\right)^2 + \left(\frac{u}{d}\right)^2\right] \bar{U} - \frac{\pi^2}{k_n} \frac{ms}{ab} \bar{V} - \frac{\pi^2 mu}{k_n\, ad} \bar{W} \tag{4.31}$$

where

$$\bar{U} = \hat{i}\, U = \hat{i} \cos \frac{m\pi x}{a} \sin \frac{s\pi y}{b} \sin \frac{u\pi z}{d} \tag{4.32}$$

$$\bar{V} = \hat{j}\, V = \hat{j} \sin \frac{m\pi x}{a} \cos \frac{s\pi y}{b} \sin \frac{u\pi z}{d} \tag{4.33}$$

$$\bar{W} = \hat{k}\, W = \hat{k} \sin \frac{m\pi x}{a} \sin \frac{s\pi y}{b} \cos \frac{u\pi z}{d} \tag{4.34}$$

$$k_n^2 = \left(\frac{m\pi}{a}\right)^2 + \left(\frac{s\pi}{b}\right)^2 + \left(\frac{u\pi}{d}\right)^2 . \tag{4.35}$$

The normalizing constants are determined by the following relationships:

$$\Lambda_n = \int_0^a \int_0^b \int_0^d |L_n|^2 \, dxdydz = \frac{abd}{\epsilon_m \epsilon_s \epsilon_u} k_n^2 \tag{4.36}$$

$$\Lambda_{n'} = \Lambda_{n''} = \int_0^a \int_0^b \int_0^d \left\{ \begin{matrix} |M_n|^2 \\ |N_n|^2 \end{matrix} \right\} dxdydz$$

$$= \Lambda_n \left[1 - \left(\frac{m\pi}{ak_n}\right)^2 \right] . \tag{4.37}$$

Substituting equations (4.29) to (4.37) into equation (4.26) and simplifying yields the following result:

$$\bar{\mathcal{G}}(\bar{r},\bar{r}_o) = \frac{4\pi}{abd} \sum_n \frac{\epsilon_m \epsilon_s \epsilon_u}{k_n^2 - k^2} \left[U(\bar{r})\, U(\bar{r}_o)\, \hat{i}\hat{i} \right.$$

$$\left. + V(\bar{r})\, V(\bar{r}_o)\, \hat{j}\hat{j} + W(\bar{r})\, W(\bar{r}_o)\, \hat{k}\hat{k} \right] . \tag{4.38}$$

The summation over n represents the triple sum over integers m, s, and u and it can be shown that

$$k_n^2 - k^2 = \left(\frac{u\pi}{d}\right)^2 - \beta_2^2 . \tag{4.39}$$

Thus the agreement between equations (4.39) and (4.22) is established.

4.6 Odd-Shaped Waveguide Problems

The ray method can also be used to solve for the Green's function for waveguides with more complicated cross-sections. The success of this approach depends on the

ability to write a general expression for the location of all the images. In many cases, the image diagram for a particular cross-section can be reduced to a superposition of image diagrams for rectangular cross-sections which are easily solvable by the ray method, as shown in section 4.2.

An example of a waveguide cross-section having an image diagram, which can be reduced in this fashion, is shown in Figure 4.4. In this diagram, the source Q_1 is located at the intersection of the medians of a right-angled isosceles triangle. For this cross-section there is no loss of generality by the assumed source location. The same image diagram results if we consider the problem of two sources, Q_1 and Q_2, located inside a square waveguide as shown by the dashed lines in Figure 4.4. This problem is easily solved in the manner of section 4.2 and thus a solution for the right triangular cross-section can be obtained.

A more complicated example to which this approach may be applied is the case of a waveguide with an equilateral triangular cross-section. The source Q_1 is again located at the intersection of the medians as shown in Figure 4.5, which is the complete image diagram for this problem. The same image diagram results by superimposing the effect of source Q_2 in the rectangular waveguide of Figure 4.6 and sources Q_3 and Q_4 in the rectangular waveguide of Figure 4.7. The boundary conditions in these figures have been

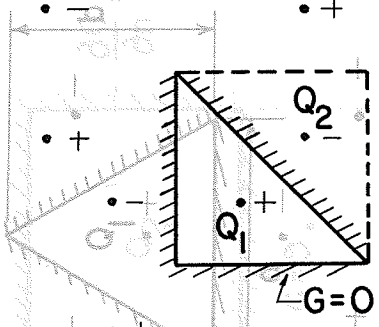

FIGURE 4.4

IMAGE DIAGRAM FOR RIGHT TRIANGULAR WAVEGUIDE

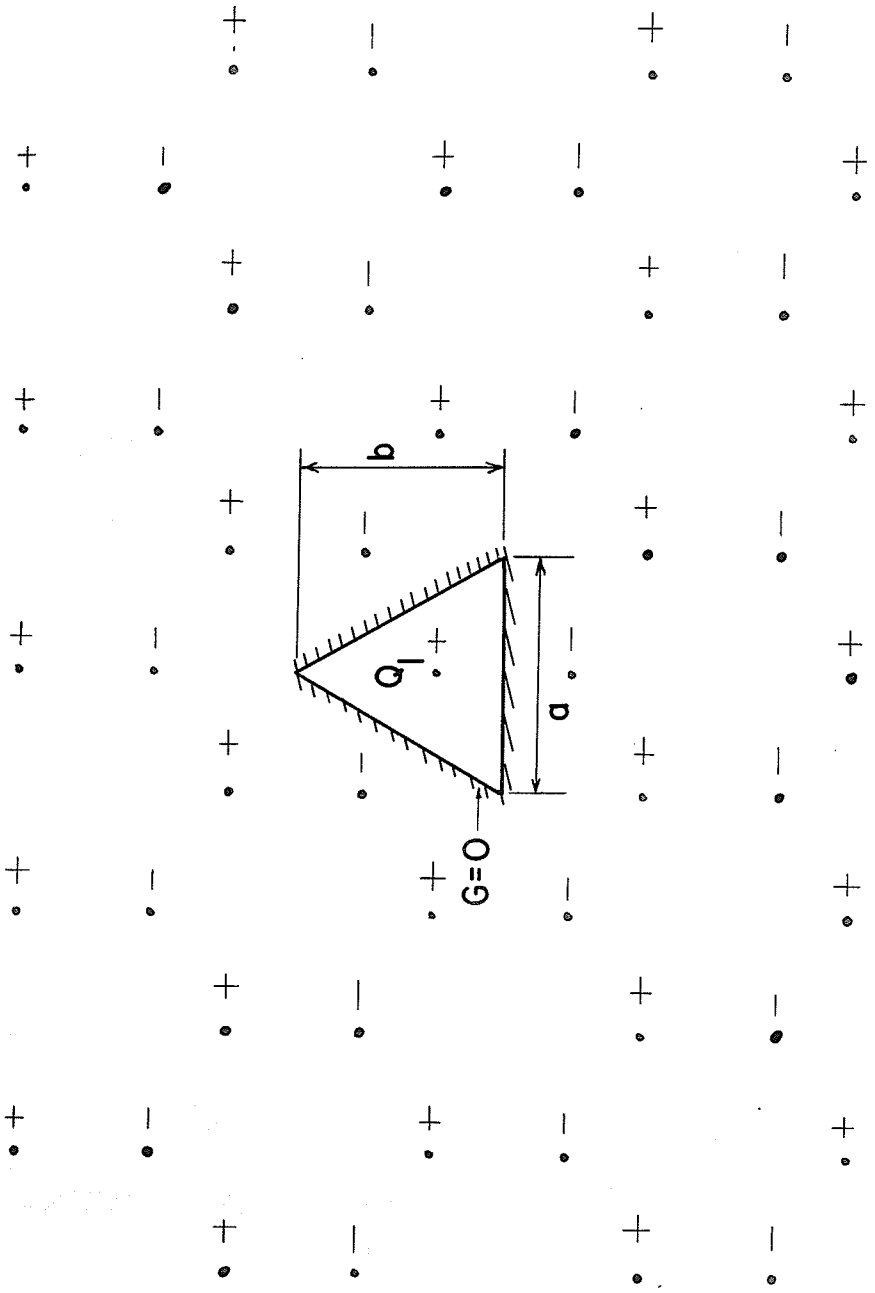

FIGURE 4.5

IMAGE DIAGRAM FOR EQUILATERAL TRIANGULAR WAVEGUIDE

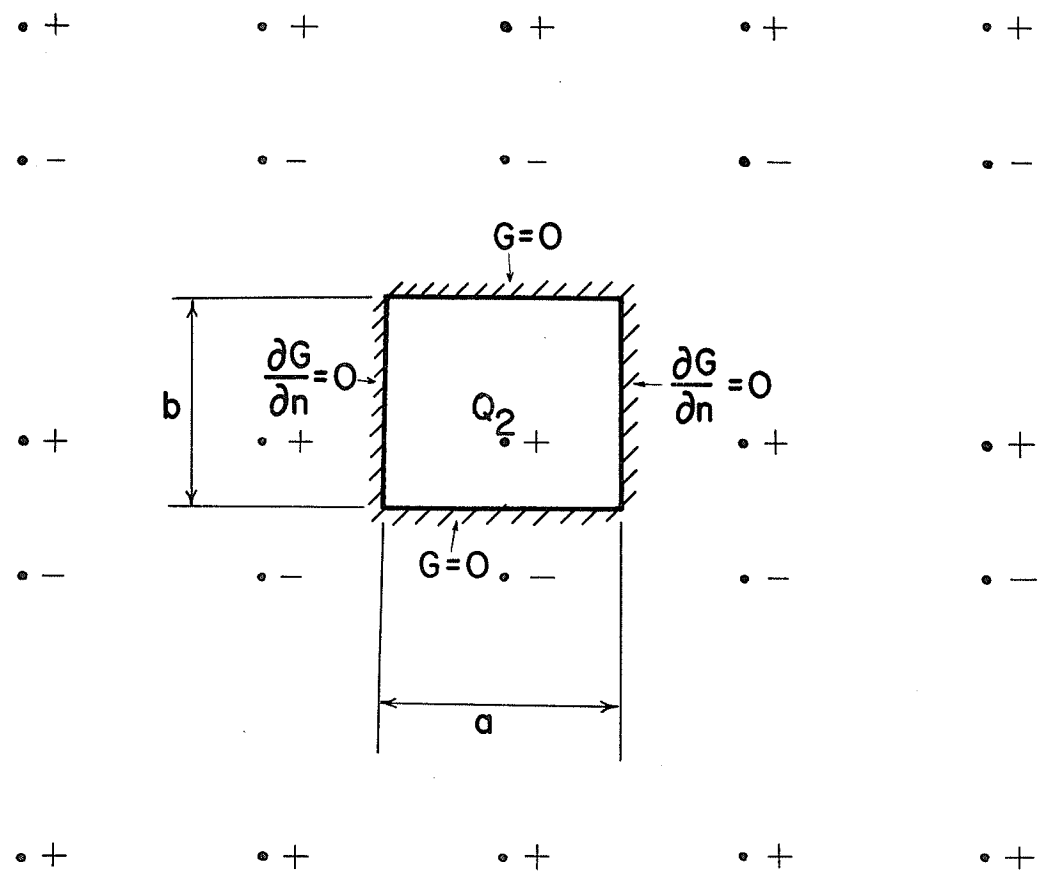

FIGURE 4.6

PARTIAL IMAGE DIAGRAM FOR EQUILATERAL TRIANGULAR WAVEGUIDE

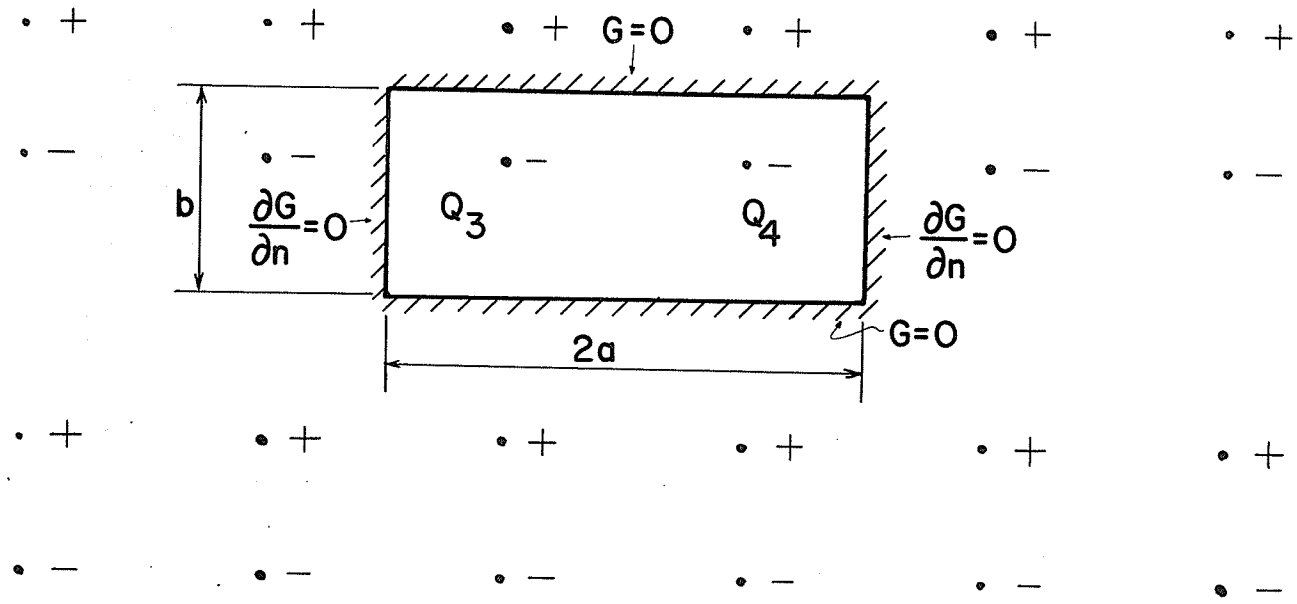

FIGURE 4.7

PARTIAL IMAGE DIAGRAM FOR EQUILATERAL TRIANGULAR WAVEGUIDE

assigned to give the correct signs for the images. These two rectangular problems are easily solved by the method of section 4.2 and thus the solution for the equilateral triangular waveguide can be found.

CHAPTER V

DISCUSSION OF RESULTS

The results derived in Chapter IV by the ray method have been shown to agree with those determined by the eigenfunction method. With the exception of the parallel plate case, our transformed ray solutions are in exact agreement with available eigenfunction solutions in spite of the approximations involved. The reasons for this agreement are discussed in this chapter.

5.1 Saddle Point Method

The principle of stationary phase is a special case of the saddle point method of integration. These techniques have been discussed by Felsen and Marcuvitz[15] and their report is applied in the following developments.

The saddle point method is applied to evaluate asymptotically, for large k, integrals of the form:

$$I_1 = \int_P f(t)\, e^{kg(t)}\, dt. \qquad (5.1)$$

where f(t) and g(t) are analytic functions of the complex variable t along the path of integration P. To evaluate I_1, the variable is changed from t to w so as to permit an easy evaluation of the integral in the w - plane:

$$I_1 = \int_{P'} F(w)\, e^{kh(w)}\, dw\,. \qquad (5.2)$$

where

$$g(t) = h(w), \tag{5.3}$$

$$F(w) = f(t)\,\frac{dt}{dw} \tag{5.4}$$

and P' is the transformation of P from the t - plane to the w - plane.

For the special case in which g(t) has one first order saddle point at t_o, i.e.:

$$g'(t_o) = o \tag{5.5}$$

$$g''(t_o) \neq o \tag{5.6}$$

and f(t) has no singularities near t_o, the pertinent change of variable is

$$g(t) = g(t_o) - w^2 . \tag{5.7}$$

The given path of integration is deformed into either a steepest descent or a constant level path through the saddle point. For complicated forms of the function g(t) the determination of the complete path may be quite difficult. Only the contribution to the integral from the neighborhood of the saddle point is considered for a first order evaluation. For the above transformation the integration along the steepest descent path is along the real w - axis and the integral in equation (5.2) becomes

$$I_1 = e^{kg(t_o)} \int_{-\infty}^{\infty} F(w)\, e^{-kw^2}\, dw . \tag{5.8}$$

If F(w) is expanded in a power series around w = o, the first term leads to the first order asymptotic approximation given by equation (3.4).

We are interested in the evaluation of a double integral by this method since in all the examples the exact solutions were produced by the asymptotic evaluation of a double integral of the form:

$$I_2 = \int_{-\infty}^{\infty} \int_{-\infty}^{\infty} f(t_1,t_2)\, e^{kg(t_1,t_2)}\, dt_1 dt_2 \,. \qquad (5.9)$$

Applying transformations as before, the following results are obtained:

$$g(t_1,t_2) = g(t_{10},t_2) - w^2 \qquad (5.10)$$

$$F(w,t_2) = f(t_1,t_2)\, \frac{dt_1}{dw} \qquad (5.11)$$

$$I_2 = \int_{-\infty}^{\infty} \int_{-\infty}^{\infty} F(w,t_2)\, e^{kg(t_{10},t_2) - kw^2}\, dt_2 dw \,. \qquad (5.12)$$

$$g(t_{10},t_2) = g(t_{10},t_{20}) - v^2 \qquad (5.13)$$

$$H(w,v) = F(w,t_2)\, \frac{dt_2}{dv} = f(t_1,t_2) \frac{dt_1}{dw}\, \frac{dt_2}{dv} \qquad (5.14)$$

$$I_2 = e^{kg(t_{10},t_{20})} \int_{-\infty}^{\infty} \int_{-\infty}^{\infty} H(w,v)\, e^{-k(w^2+v^2)}\, dw\, dv. \qquad (5.15)$$

The function H(w,v) is expanded in a Taylor series

around $w = v = o$, the first term of which is

$$H(o,o) = f(t_{10},t_{20}) \left[\frac{dt_1}{dw} \frac{dt_2}{dv}\right]_{w=v=o} \tag{5.16}$$

The integration of this term leads to exact solutions for the cases considered in Chapter IV. Either the sum of the following terms or else the integral of this sum must vanish. The determination of the higher order terms in the expansion of $H(w,v)$ is an extremely lengthy process. If a complete general expansion of this function could be found it might be possible to establish a set of conditions on the functions $f(t_1,t_2)$ and $g(t_1,t_2)$ for which this method would result in exact solutions. Another possible approach would be to find a set of conditions for which the right hand side of equation (5.15) with $H(w,v)$ replaced by $H(o,o)$ satisfies the wave equation. All attempts to establish these conditions have so far failed.

5.2 Form of the Solution

It is well known that solutions of the Helmholtz equation in separable coordinates can be written as the product of eigenfunctions. The first term in the asymptotic expansion of this solution can be found by applying ray theory and saddle point integration techniques as discussed previously. An illustration of this is the parallel plate case presented in Chapter IV, which has an eigenfunction

solution of the form:

$$G(\bar{r},\bar{r}_o) = -\frac{2\pi}{a} j \sum_{m=1}^{\infty} H_o^{(2)}(\beta r) \sin\frac{m\pi}{a}x \sin\frac{m\pi}{a}x_o \qquad (5.17)$$

where

$$\beta^2 = k^2 - \left(\frac{m\pi}{a}\right)^2 .$$

It is easily seen that the first term in the asymptotic expansion of this solution, for large kr, is the right hand side of equation (4.7) which was derived by the ray method as shown in section 4.1. The sine and cosine functions remain unchanged in the expansion. For all the other cases presented in Chapter IV, the exact solution is the product of exponential functions and therefore the asymptotic approach results in the exact solutions. Another example of this is done in Appendix D where the solution for a line source between parallel plates is determined using the principle of stationary phase in conjunction with the image method and Poisson sum formula. The solution obtained in this manner is found to agree with the exact solution derived by Morse and Feshbach.

Thus it is seen that when the solution for a guiding system with separable coordinates is expressible in terms of exponential functions, the application of the asymptotic techniques described previously results in the exact solution.

CHAPTER VI

CONCLUSIONS

A systematic procedure to evaluate the Green's function by converting the ray field into modal form using the Poisson sum formula has been presented. In the examples, the ray fields were determined by using the image method. When this method is applicable and a point source is considered, the ray formulation of the Green's function is exact. If these conditions do not hold, then an asymptotic ray solution can be found using Keller's geometrical theory of diffraction. In principle, the conversion from rays to modes can be carried out in all cases by using the Poisson sum formula. The procedure to convert into mode form requires the evaluation of the Fourier transform of the ray fields, as discussed in Chapter V, these integrals may sometimes be difficult to evaluate but for certain special cases they can easily be evaluated exactly by asymptotic techniques. The conditions on the integrand for which the asymptotic integration produces exact results have not as yet been determined. A more detailed investigation into this problem would definitely be worthwhile.

This thesis establishes the ray method as a technique for determining the Green's function for guiding structures in which the wave equation may be separated, and gives a physical insight into the mechanisms of propagation in

these structures. While the eigenfunction method is easier for simple geometries, the ray method can easily be applied to problems involving discontinuities in the structure[1], curvature of the walls, or bending of the axis of symmetry. The ray field in a circular waveguide could be determined by considering the superposition of an infinite number of wedges, for which an exact solution is known, located around the circumference of the waveguide. The ray method is also applicable to solve scattering of various bodies inside waveguides and cavities in terms of elementary functions.

APPENDICES

APPENDIX A

THREE DIMENSIONAL POISSON SUM FORMULA

For a single summation it has been shown that the following relationships hold:(12)

$$\sum_{n=-\infty}^{\infty} f(2\pi n) = \frac{1}{\sqrt{2\pi}} \sum_{m=-\infty}^{\infty} F(m) \tag{A.1}$$

$$F(m) = \frac{1}{\sqrt{2\pi}} \int_{-\infty}^{\infty} f(t)\, e^{-jmt}\, dt. \tag{A.2}$$

The Poisson sum formula can be extended to deal with double and triple infinite sums. By a step by step application of the above formulae to a triple sum over indices n, p, and q the transformation to a triple sum over new indices m, s, and u is achieved. The new function F(m,s,u) is found to be the three dimensional Fourier transform of the original function $f(2\pi n, 2\pi p, 2\pi q)$.

We consider the sum over the infinite ranges of n, p, and q:

$$\sum_n \sum_p \sum_q f(2\pi n, 2\pi p, 2\pi q). \tag{A.3}$$

Applying equations (A.1) and (A.2) to expression (A.3) yields the following equations:

$$\sum_q f(2\pi n, 2\pi p, 2\pi q) = \frac{1}{\sqrt{2\pi}} \sum_u F_3(u) = f_3(2\pi n, 2\pi p) \tag{A.4}$$

$$F_3(u) = \frac{1}{\sqrt{2\pi}} \int_{-\infty}^{\infty} f(2\pi n,\ 2\pi p,\ t_3)\ e^{-jut_3}\ dt_3 \qquad (A.5)$$

$$\sum_p f_3(2\pi n,\ 2\pi p) = \frac{1}{\sqrt{2\pi}} \sum_s F_2(s) = f_2(2\pi n) \qquad (A.6)$$

$$F_2(s) = \frac{1}{\sqrt{2\pi}} \int_{-\infty}^{\infty} f_3(2\pi n,\ t_2)\ e^{-jst_2}\ dt_2 \qquad (A.7)$$

$$\sum_n f_2(2\pi n) = \frac{1}{\sqrt{2\pi}} \sum_m F_1(m) \qquad (A.8)$$

$$F_1(m) = \frac{1}{\sqrt{2\pi}} \int_{-\infty}^{\infty} f_2(t_1)\ e^{-jmt_1}\ dt_1 \qquad (A.9)$$

$$\sum_n f_2(2\pi n) = \sum_n \sum_p f_3(2\pi n,\ 2\pi p)$$

$$= \sum_n \sum_p \sum_q f(2\pi n,\ 2\pi p,\ 2\pi q) \qquad (A.10)$$

$$\sum_m F_1(m) = \sum_m \frac{1}{\sqrt{2\pi}} \int_{-\infty}^{\infty} f_2(t_1)\ e^{-jmt_1}\ dt_1 \qquad (A.11)$$

Substituting for $f_2(t_1)$ and then again for $f_3(t_1,t_2)$ in equation (A.11) and rearranging leads to the final result.

$$\sum_n \sum_p \sum_q f(2\pi n,\ 2\pi p,\ 2\pi q) = \sum_m \sum_s \sum_u \frac{1}{(2\pi)^3}\ .$$

$$f(t_1,t_2,t_3)\, e^{-j(mt_1+st_2+ut_3)}\, dt_1 dt_2 dt_3 \qquad (A.12)$$

All summations are taken over the range from minus infinity to plus infinity.

APPENDIX B

EVALUATION OF A DOUBLE INTEGRAL BY METHOD OF STATIONARY PHASE

In general the double integrals, which were evaluated in Chapter IV for the rectangular waveguides and cavity, were of the form

$$\int_{-\infty}^{\infty}\int_{-\infty}^{\infty} \frac{e^{-jk\left[(x-t_1\frac{a}{\pi})^2 + (y-t_2\frac{b}{\pi})^2 + z^2\right]^{1/2} - j(mt_1+st_2)}}{\left[(x-t_1\frac{a}{\pi})^2 + (y-t_2\frac{b}{\pi})^2 + z^2\right]^{1/2}} dt_1 dt_2 .$$

This integral can be evaluated by successive application of equation (3.4) or by direct application of equation (3.5). The two methods are identical and the use of equation (3.5) gives the following equations:

$$f(t_1,t_2) = \left[(x-t_1\frac{a}{\pi})^2 + (y-t_2\frac{b}{\pi})^2 + z^2\right]^{-1/2} \qquad (B.1)$$

$$g(t_1,t_2) = -\left[(x-t_1\frac{a}{\pi})^2 + (y-t_2\frac{b}{\pi})^2 + z^2\right]^{1/2} - \frac{mt_1}{k} - \frac{st_2}{k} . \qquad (B.2)$$

The solution of $\partial g/\partial t_1 = \partial g/\partial t_2 = o$ gives the two stationary phase points:

$$t_{10} = \frac{\pi}{a}\left[x - \frac{m\pi}{\beta_2 a}|z|\right] \qquad (B.3)$$

$$t_{20} = \frac{\pi}{b}\left[y - \frac{s\pi}{\beta_2 b}|z|\right] \qquad (B.4)$$

where

$$\beta_2^2 = k^2 - \left(\frac{m\pi}{a}\right)^2 - \left(\frac{s\pi}{b}\right)^2 . \qquad (B.5)$$

Evaluating the terms in equation (3.5) yields:

$$\alpha = \frac{\partial^2 g}{\partial t_1^2}\bigg|_{(t_{10},t_{20})} = -\frac{a^2\beta_2}{\pi^2 zk^3}\left[k^2 - \left(\frac{m\pi}{a}\right)^2\right] \qquad (B.6)$$

$$\beta = \frac{\partial^2 g}{\partial t_2^2}\bigg|_{(t_{10},t_{20})} = \frac{-b^2\beta_2}{\pi^2 zk^3}\left[\beta_2^2 + \left(\frac{m\pi}{a}\right)^2\right] \qquad (B.7)$$

$$\gamma = \frac{\partial^2 g}{\partial t_1 \partial t_2}\bigg|_{(t_{10},t_{20})} = \frac{ms\beta_2}{zk^3} \qquad (B.8)$$

$$g(t_{10},t_{20}) = -\frac{m\pi}{ka}x - \frac{s\pi}{kb}y - \frac{\beta_2}{k}|z| \qquad (B.9)$$

$$f(t_{10},t_{20}) = \frac{\beta_2}{zk} . \qquad (B.10)$$

Therefore the double integral becomes:

$$-\frac{2\pi^3 j}{ab\beta_2}\, e^{-j\left(\frac{m\pi x}{a} + \frac{s\pi y}{b} + \beta_2 |z|\right)} . \qquad (B.11)$$

The above expression is used to construct the final mode solution for the rectangular structures in Chapter IV as outlined there.

APPENDIX C

EVALUATION OF INTEGRAL (4.19)

The integral (4.19) which arises in the transformation of rays to modes for the rectangular cavity is of the following form:

$$I = \int_{-\infty}^{\infty} e^{-j\beta_2 \left| z - t_3 \frac{d}{\pi} \right| - jut_3} \, dt_3 \, . \qquad (C.1)$$

Splitting the range of integration yields:

$$I = \int_{-\infty}^{z\frac{\pi}{d}} e^{-j\left[\beta_2 z + (u - \frac{d}{\pi}\beta_2)\, t_3\right]} dt_3$$

$$+ \int_{z\pi/d}^{\infty} e^{-j\left[-\beta_2 z + (\frac{d}{\pi}\beta_2 + u)\, t_3\right]} dt_3 . \qquad (C.2)$$

By the change of variable $v = t_3 - z\frac{\pi}{d}$, we get:

$$I = -e^{-j\beta_2 z} \int_{\infty}^{0} e^{-j\beta_2 \left(\frac{u}{\beta_2} - \frac{d}{\pi}\right)\left(v + z\frac{\pi}{d}\right)} dv$$

$$+ e^{j\beta_2 z} \int_{0}^{\infty} e^{-j\beta_2 \left(\frac{u}{\beta_2} + \frac{d}{\pi}\right)\left(v + \pi\frac{z}{d}\right)} dv . \qquad (C.3)$$

Integrating with respect to v gives:

$$I = \frac{e^{-ju\frac{\pi}{d}z}}{-j\beta_2\left(\frac{u}{\beta_2} - \frac{d}{\pi}\right)} + \frac{e^{-ju\frac{\pi}{d}z}}{j\beta_2\left(\frac{u}{\beta_2} + \frac{d}{\pi}\right)} . \qquad (C.4)$$

Simplifying, the integral becomes:

$$I = \frac{2j\beta_2\,\pi}{d\left[\left(\frac{u\pi}{d}\right)^2 - \beta_2^{\,2}\right]}\; e^{-j\frac{u\pi z}{d}} \quad . \qquad (C.5)$$

APPENDIX D

LINE SOURCE BETWEEN PARALLEL PLATES

The method of images was used by Morse and Feshbach[12] to determine the Green's function for a line source between infinite conducting parallel plates with separation h. The two dimensional Green's function of equation (2.9) was used and the ray solution was transformed into the mode solution by the Poisson sum formula. The Fourier transform of the ray fields was determined exactly by contour integration. In this appendix an alternate way of arriving at the same solution is presented.

The solution is formed as done by Morse and Feshbach by imaging and applying the Poisson sum formula, resulting in the following Fourier integral:

$$I = \int_{-\infty}^{\infty} e^{-jmt_1} \left\{ H_o^{(1)} \left[k \sqrt{(x-x_o-t_1\frac{h}{\pi})^2 + (y-y_o)^2} \right] + H_o^{(1)} \left[k \sqrt{(x+x_o-t_1\frac{h}{\pi})^2 + (y-y_o)^2} \right] \right\} dt_1 \qquad (D.1)$$

Note that Morse and Feshbach suppress exp $(-j\omega t)$ and for all other cases in this thesis exp $(j\omega t)$ has been suppressed. This difference results in the use of $H_o^{(1)}(kr)$ instead of $H_o^{(2)}(kr)$ for this problem.

This integral can be evaluated by writing $H_o^{(1)}(kr)$ in integral form and then using equation (3.5). Application of an asymptotic method of integration to the Hankel function

results in the first term of its asymptotic expansion.[19] When this is substituted into equation (D.1) the result is:

$$I \sim \int_{-\infty}^{\infty} e^{-jmt_1} \left(\frac{2}{\pi k}\right)^{1/2} e^{-j\frac{\pi}{4}} \left\{ \frac{e^{jkr_1}}{r_1^{1/2}} + \frac{e^{jkr_2}}{r_2^{1/2}} \right\} dt_1 \qquad (D.2)$$

where

$$r_1^2 = (x-x_o-t_1\frac{h}{\pi})^2 + (y-y_o)^2$$

$$r_2^2 = (x+x_o-t_1\frac{h}{\pi})^2 + (y-y_o)^2 \ .$$

Evaluation of the integral in equation (D.2) by stationary phase in exactly the same manner as done for equation (4.2) yields:

$$I = \frac{4\pi}{h\sqrt{k^2-(\frac{m\pi}{h})^2}} \cos\frac{m\pi x_o}{h} \ e^{-j\frac{m\pi}{h}x + j\sqrt{k^2-(\frac{m\pi}{h})^2}\,|y-y_o|} . \qquad (D.3)$$

This result agrees with the exact solution found by Morse and Feshbach. This is then another illustration of the application of the asymptotic method of integration to produce exact solutions.

It is of interest to note that the equation (D.2) could have been produced directly by using the asymptotic form of the two dimensional source that is used in Keller's ray theory.

BIBLIOGRAPHY

BIBLIOGRAPHY

1. Hamid, M. A. K., "Near Field Transmission Between Horn Antennas", Research Report. No. 43, Department of Electrical Engineering, University of Toronto, April 1966, Appendices A2.2 and A3.6.

2. Pekeris, C. L., "Ray Theory vs. Normal Mode Theory in Wave Propagation Problems", Proceedings of Symposia in Applied Mathematics, Vol. II, Electromagnetic Theory, Am. Math. Soc., 1950, pp. 71-75.

3. Morse, P. M., Feshbach, H., "Methods of Theoretical Physics", McGraw-Hill Book Company, 1953, Part I, pp. 812-820.

4. Collin, R. E., "Field Theory of Guided Waves", McGraw-Hill Book Company, 1960, Chapter 2.

5. Morse, Feshbach, op. cit., Part II, Chapter 13.

6. Ibid., Part I, pp. 808-811.

7. Keller, J. B., "The Scope of the Image Method" Communications on Pure and Applied Mathematics, Vol. 6, 1953, pp. 505-512.

8. Keller, J. B., "Geometrical Theory of Diffraction", Journal of the Optical Society of America, Vol. 52, No. 2, February 1962, pp. 116-130.

9. Morse, Feshbach, op. cit., Part I, Section 1.6.

10. Brekhovskikh, L. M., "Waves in Layered Media", Academic Press, 1960, Chapter V, Sections 25 and 26.

11. Titchmarsh, E. C., "Introduction to the Theory of Fourier Integrals", Oxford University Press, 1937, p. 61.

12. Morse, Feshbach, op. cit., Part I, pp. 466-467.

13. Copson, E. J., "Asymptotic Expansions", Cambridge at the University Press, 1965.

14. Erdelyi, A., "Asymptotic Expansions", Dover Publications, Inc., 1956.

15. Felsen, L. B., Marcuvitz, N., "Modal Analysis and Synthesis of Electromagnetic Fields", P. I. B. Microwave Research Institute, Research Report R-776-59, P. I. B. - 705, October 1959.

16. Born, M., Wolf, E., "Principles of Optics", Third Edition, Pergamon Press, 1965, Appendix III.

17. Collin, op. cit., pp. 198-200.

18. Ibid., pp. 262-264.

19. Watson, G. N., "A Treatise on the Theory of Bessel Functions", Second Edition, Cambridge at the University Press, 1962, Chapter 7.